

Novel Receiver for Superparamagnetic Iron Oxide Nanoparticles in a Molecular Communication Setting

Max Bartunik*
 Maximilian Luebke*
 max.bartunik@fau.de
 maximilian.luebke@fau.de
 Institute for Electronics Engineering
 Friedrich-Alexander-University
 Erlangen-Nuernberg (FAU)
 Erlangen, Germany

Harald Unterweger
 Christoph Alexiou
 Section of Experimental Oncology
 and Nanomedicine (SEON)
 University Hospital Erlangen
 Erlangen, Germany

Sebastian Meyer
 Doaa Ahmed
 Georg Fischer
 Institute for Electronics Engineering
 FAU, Erlangen, Germany

Wayan Wicke
 Vahid Jamali Kooshkghazi
 Robert Schober
 Institute for Digital Communication
 FAU, Erlangen, Germany

Jens Kirchner
 jens.kirchner@fau.de
 Institute for Electronics Engineering
 FAU, Erlangen, Germany

ABSTRACT

Superparamagnetic iron oxide nanoparticles (SPIONs) have recently been introduced as information carriers in a testbed for molecular communication (MC) in duct flow. Here, a new receiver for this testbed is presented, based on the concept of a bridge circuit. The capability for a reliable transmission using the testbed and detection of the proposed receiver was evaluated by sending a text message and a 80 bit random sequence at a bit rate of 1/s, which resulted in a bit error rate of 0 %. Furthermore, the sensitivity of the device was assessed by a dilution series, which gave a limit for the detectability of peaks between 0.1 to 0.5 mg/mL. Compared to the commercial susceptometer that was previously used as receiver, the new detector provides an increased sampling rate of 100 samples/s and flexibility in the dimensions of the propagation channel. Furthermore, it allows to implement both single-ended and differential signaling in SPION-bases MC testbeds.

KEYWORDS

Molecular communication, superparamagnetic iron oxide nanoparticles, SPION, differential signaling, receiver

ACM Reference Format:

Max Bartunik, Maximilian Luebke, Harald Unterweger, Christoph Alexiou, Sebastian Meyer, Doaa Ahmed, Georg Fischer, Wayan Wicke, Vahid Jamali Kooshkghazi, Robert Schober, and Jens Kirchner. 2019. Novel Receiver for

Superparamagnetic Iron Oxide Nanoparticles in a Molecular Communication Setting. In *ACM NanoCom 2019: 6th ACM International Conference on Nanoscale Computing and Communication, September 25–27, 2019, Dublin, Ireland*. ACM, New York, NY, USA, 6 pages. <https://doi.org/10.1145/1122445.1122456>

1 INTRODUCTION

In the exploration of molecular communication strategies (see [6, 10] for an overview), testbeds play a central role as they allow to evaluate communication theory, to identify new physical aspects that have to be taken into account such as sources of interference and to provide steps towards implementation of molecular communication for practical systems applications.

For that purpose, testbeds have been proposed based on alcohol [3, 7] (see also [12] for spatial instead of temporal coding) and acids/bases [4] (refer to [5, 8] for corresponding transmitter and receiver designs) as signaling molecules. A third type of information carrier was proposed by the authors in [11] for a testbed based on superparamagnetic iron oxide nanoparticles (SPIONs). In contrast to alcohol and acids/bases, these particles, which were originally developed for magnetic drug delivery, are biocompatible and hence applicable for use in humans. They can be fabricated relatively easily and are detected as a change in inductance of a measurement coil wound around the propagation channel. Hence, detectors can be operated noninvasively, i. e., they do not have to be inserted into the propagation channel, which provides a major advantage for human use, e. g., with blood vessels as propagation channel.

However, a major challenge when implementing testbeds for MC is the lack of appropriate detectors. In the present case, the receiver that was used in [11], the commercial susceptometer Bartington® MS2G, was not operated according to its original measurement purpose, i. e., the characterization of material samples. It therefore exhibited two considerable disadvantages: First, the detector coil had a fixed width. This, on the one hand, posed restrictions on the maximum width of the propagation channel. On the other hand, for channel widths smaller than the detector width, enhancement

*Both authors contributed equally to this research.

Permission to make digital or hard copies of all or part of this work for personal or classroom use is granted without fee provided that copies are not made or distributed for profit or commercial advantage and that copies bear this notice and the full citation on the first page. Copyrights for components of this work owned by others than ACM must be honored. Abstracting with credit is permitted. To copy otherwise, or republish, to post on servers or to redistribute to lists, requires prior specific permission and/or a fee. Request permissions from permissions@acm.org.

ACM NanoCom 2019, September 25–27, 2019, Dublin, Ireland

© 2019 Association for Computing Machinery.

ACM ISBN 978-1-4503-9999-9/18/06...\$15.00

<https://doi.org/10.1145/1122445.1122456>

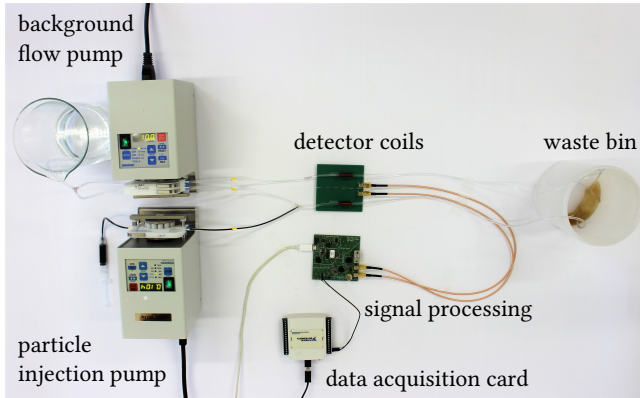


Figure 1: Testbed. From left to right are shown: Transmitter consisting of water reservoir for background flow, syringe as reservoir for particle injection, two pumps for providing the background flow and the particle injection (upper and lower pump, respectively) and Y-connector; propagation channel after the Y-connector; receiver consisting of the PCB's for detector coils and signal processing (upper and lower PCB, respectively), data acquisition card and waste bin.

of the measurement signal and thus of the detector sensitivity by reducing the width of the detector coil was not possible. Second, the susceptometer, which is not intended for dynamic measurements, provided a maximum sample rate of only 10 samples/s. Hence, in order to achieve higher flexibility in the dimensions of the propagation channel and to increase both the temporal and the measurement resolution, a new customized detector device for SPION-based MC is needed. In this paper, a first prototype of this device is presented.

The proposed device offers yet another feature: It incorporates a second coil to provide a reference signal. Hence, the detector can not only be operated in a single-ended signaling design with one propagation channel as in previous testbeds for molecular communication, but can also be used for a differential signaling design, where information is encoded in the difference of SPIONs concentration between two tubes that serve as propagation channel.

In the following sections, the testbed will be outlined (for more details, see [11]) and the design of the proposed detector will be described. The device is evaluated by transmitting an exemplary text message and by assessing its sensitivity for different concentrations of SPION solutions. A discussion of the achievements and potential future applications concludes the article.

2 TESTBED

Figure 1 shows the complete testbed including the propagation channel.

2.1 Information Carriers

Information is encoded in the SPION concentration in aqueous solution: A binary “1” is represented by the injection of SPION particles into the propagation channel, a binary “0” by no particles being released.

SPIONs originate from biomedical applications and thus have an established biocompatibility with ongoing studies on biosafe applications [9]. The nanoparticles used as transmitter molecules in this setup were synthesized by the Section of Experimental Oncology and Nanomedicine (SEON) of the University Hospital Erlangen. They have a hydrodynamic radius of 50 nm and a susceptibility of 8.78×10^{-3} for 1 mg/mL. They are suspended in water with an estimated particle concentration of 5×10^{13} particles/mL for a stock concentration of 10 mgFe/mL.

2.2 Transmitter

The transmitter consists of the following components: a reservoir with distilled water, which together with a first pump (Ismatec® ISM831C) provides the channel medium in form of a background flow with a continuous rate of 10 mL/min; a syringe as reservoir for the SPION suspension; a second, computer controlled pump (Ismatec® ISM596D) that injects a defined amount of this SPION suspension into the transmission channel. For that purpose, the tubes for background flow and particle injection are joined via a Y-connector. The pump for SPION injection is controlled with a LabView application that allows to encode the desired binary sequence in a series of particle releases, each with a volume of 104 μ L and at a flow rate of 10 mL/min. A symbol duration of 1 s was employed.

2.3 Propagation Channel

The propagation channel consists of a tube with a diameter of 0.84 mm and a length of 5 cm. The channel begins after the Y-connector that joins background flow and particle injection and ends at the detector coil of the receiver.

2.4 Receiver

The bursts of SPIONs traveling through the propagation channel are measured with a detector coil as the SPIONs change the inductance value of the coil while they pass through it. This basic principle is exploited in magnetic susceptometers [1]. In this paper, the commercial susceptometer that was used in previous studies [11] (Bartington MS2G) is replaced by the device described in the following section.

3 DEVICE CONCEPTION AND REALIZATION

As in the previously used, commercial susceptometer, the nanoparticle are detected by a change of inductance of a coil that they pass through. For the proposed design, two coils within a bridge circuit are utilized, one as reference and one for measurement [2, ch. 32]. Combined with an appropriate capacitor each coil forms a resonator circuit that is driven by an amplified generator signal. SPIONs passing through the measurement coil cause a change in inductance and as a consequence also a shift in resonance frequency. As a result the bridge circuit is unbalanced and the resulting differential voltage is detected via an instrumentation amplifier and digital processing.

3.1 Power Supply

To amplify the generator signal and for use in the instrumentation amplifier, operational amplifiers that are driven by a differential

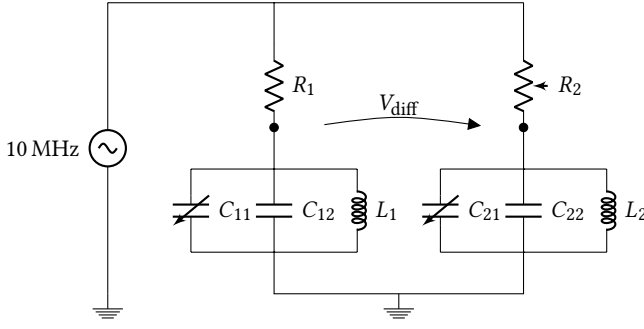


Figure 2: Bridge circuit. The tunable capacitances C_{11} , C_{21} and tunable resistance R_2 are used to balance the bridge during calibration. SPIONs that flow through the detector coil change its inductance (either L_1 or L_2), which results in a non-zero voltage difference V_{diff} .

power source (± 5 V and ± 15 V) were selected. To simplify the external power supply, all required voltages are produced by the device from a single 5 V source.

To supply the required ± 15 V voltage from the 5 V source, the split-rail converter TPS65131 (Texas Instruments) was used. The -5 V rail was provided by reducing the -15 V output via a negative voltage regulator (LM79L05, Texas Instruments).

3.2 Signal Generator

The resonator circuit is driven by a sine wave source with a frequency of 10 MHz, namely the ultra-low phase noise sine wave generator CVSS-945-10000 by Crystek. The voltage-tunable output frequency was set to 10 MHz by means of a 2.5 V low-dropout regulator (LP5907, Texas Instruments). A load of 50Ω was connected to the signal output, resulting in a peak-to-peak voltage of 3 V.

As a higher voltage swing is desired, a current feedback amplifier (LT1223, Linear Technology) with a large output drive and a gain bandwidth of 100 MHz was used to amplify the generated signal to a peak-to-peak voltage of approximately 15 V. As the optimal amplification factor was determined during testing, a potentiometer was fitted to adjust the resulting output voltage.

3.3 Bridge Circuit

A bridge circuit, typically consisting of four impedances, is implemented here with two resistors and the resonator circuits for the detector coils as shown in Fig. 2. A potentiometer is used as resistor R_2 and both branches contain adjustable capacitances (C_{11} and C_{21}) to allow tuning of the resonance frequency. Simple switching of detector coils is enabled by use of SMA- (SubMiniature version A) headers.

Ideally, if correctly tuned, the voltage V_{diff} between the two branches of the bridge circuit is zero as long as no nanoparticles pass through the detector coils. As soon as a difference in inductance of one coil (either L_1 or L_2) occurs the corresponding resonator circuit will be de-tuned, the impedance changes, and the branches of the bridge become unbalanced.

By tuning the branches of the bridge circuit equally, a peak-to-peak difference voltage V_{diff} below 40 mV could be achieved. This

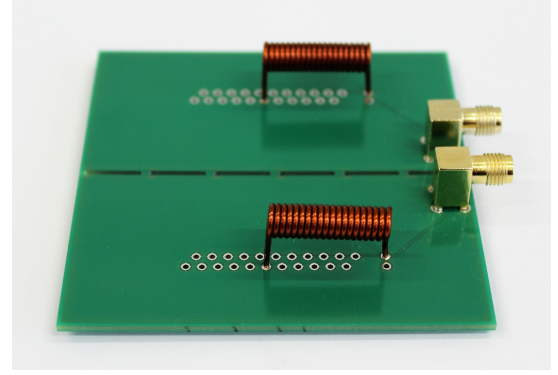


Figure 3: Detector coils mounted on PCB

value hence constitutes the limit of tunability of the two branches by use of the tunable resistor and capacitances.

3.4 Detector Coils

To fit the requirements and geometry of the setup ideally, special detector coils were produced. They have an inner diameter that allows a tube with a girth of up to 3.5 mm to be exchanged easily without a needlessly large air gap remaining. To this end, bondable enamelled wire with a diameter of 1 mm was wound around a steel rod (4 mm) to produce a coil of approximately 20 mm length with 20 windings. The coil was heated thoroughly under a hot air flow to bond the individual windings, ensuring mechanical stability and therefore a constant inductance value.

For reasons of usability the produced coils were mounted on a printed circuit board (PCB) and attached to SMA headers (see Fig. 3).

3.5 Instrumentation Amplifier

To simplify the detection of voltage level changes in the bridge circuit, an instrumentation amplifier was implemented using two current feedback amplifiers of the type LT1395 from Linear Technology as input stage and the operation amplifier AD8033 from Analog Devices as amplification stage. The chosen devices show low noise over a sufficient bandwidth. The differential amplification of the instrumentation amplifier can be adjusted with a potentiometer.

The maximal amplification factor in the real-life application was limited by the current the power source could provide. After tuning the branches of the bridge circuit, the amplification of the instrumentation amplifier was adjusted to an output peak-to-peak voltage of 1 V.

3.6 Digital Measurement

A simple digital measurement is made possible through an envelope detector connected to the output of the instrumentation amplifier. The result is a DC-signal that varies in the range of 100 to 500 mV. The output signal was captured with the data acquisition module NI USB-6009 from National Instruments. The module has a resolution of 11 bit with a programmable-gain amplifier and a maximal sample rate of 10^4 samples/s. The supplied LabView application “NI-DAQmx Base Data Logger” was used to digitally record

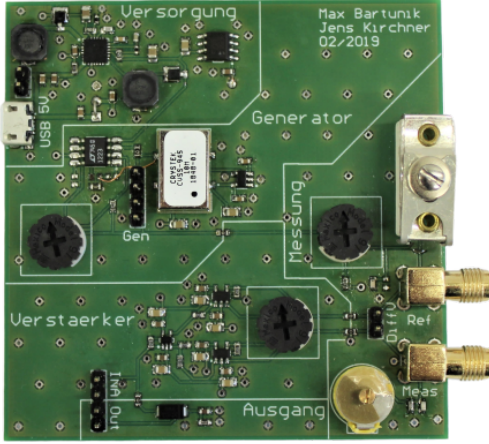


Figure 4: Signal acquisition circuitry.

measured values. A sample rate of 100 samples/s was used for all measurements.

3.7 Printed Circuit Board

The described circuitry was implemented on a four layered PCB consisting of 1.55 mm thick FR-4 composite material with a square layout of 75 mm by 75 mm. Layers two and four, consisting solely of ground planes, act as shielding. Layer 1 contains the signal components, while the power distribution is implemented in layer 3. All remaining space is covered with ground planes and connected through a mesh of vias. Additionally, a via is placed closed to every surface mounted device (SMD) with a ground connection. Figure 4 shows the completely assembled detector device.

Altium Designer 18.1.7 was used to layout the PCB, which was produced by the Multi Leiterplatten GmbH, Germany, and assembled with the own department facilities.

3.8 Tuning Procedure

Balancing the bridge circuit is an important step for the functionality of the device. To maximize the sensitivity as SPIONs pass through the detector coil, the resonator circuits should ideally be in resonance at 10 MHz and identical to each other. Due to small differences in the inductance of the detector coils, a trade-off between ideal resonance and identical resonance must be found.

In the first step, the PCB was fitted with SMD capacitances (C_{12} and C_{22} in Fig. 2) that shifted the resonance frequency into the desired range. The tunable capacitances C_{11} and C_{21} were then adjusted to maximize the signal output of each channel and therefore maximize resonance. Using the potentiometer R_2 , the peak-to-peak voltage of both channels was matched. Finally, to compensate for the influence of the used measurement tips, with a given capacitance of 16 pF, the tuning steps were repeated while measuring the output of the instrumentation amplifier, which in turn was adjusted to a peak-to-peak voltage of 1 V. All measurements were performed with the oscilloscope WaveRunner LT262 (LeCroy).

4 DEVICE EVALUATION

The proposed measurement device was evaluated in two respects: As a proof of concept, a simple text message was sent with the testbed. Furthermore, the sensitivity of the device was assessed by comparing pulse series with different concentrations of SPION suspension.

4.1 Text Message Transmission and Long Random Binary Sequence

A simple coding table was devised to transmit text messages composed of capital letters efficiently. Each codeword is headed by a logical “1” to allow receiver synchronization, followed by 5 bit representing the character to be coded. This latter code component is the 5-bit binary representation of the number of the letter within the Latin alphabet, starting with zero for letter “A”. Hence,

$$“A” \equiv “100000”, \quad “B” \equiv “100001”, \quad \dots$$

$$“F” \equiv “100101”, \quad \dots$$

$$“U” \equiv “110100”, \quad \dots$$

With this coding scheme, the sample sequence “FAU” with binary representation

$$100101 \ 100000 \ 110100 \quad (1)$$

was transmitted using a suspension with a particle concentration of 7.5 mg/mL.

At the receiver, peak detection was performed by use of Matlab (MathWorks), before decoding the bit sequence. First noise in the received data was reduced by applying a moving average filter with a width of 21 samples. Next, a threshold to differentiate between the logical values “1” and “0” was calculated from the received data as the mean between the highest and the lowest value. Finally, the rising edges were identified as threshold-crossings with positive slope. Based on the time t_0 of the first detected rising edge and symbol interval T_S , symbol intervals were defined by (for interval no. k)

$$I_k = [t_0 + kT_S; t_0 + (k + 1)T_S[\quad (2)$$

Bit no. k was set to “1” if the threshold was exceeded for at least 30 % of samples in I_k , and to “0” otherwise.

A further test with a random sequence of 80 bit was performed:

$$\begin{aligned} &11001001 \ 11111110 \ 10110011 \ 01101000 \ 10001010 \\ &01011001 \ 01100011 \ 11111000 \ 11010101 \ 00001000 \end{aligned} \quad (3)$$

4.2 Sensitivity Test

To characterize the quality of detection and allow for comparison to other devices, the sensitivity of the receiver was determined. To this end, the bit sequence “10101” was transmitted using various dilutions of the SPION suspension. Solutions with a particle concentration of 10 mg/mL, 5.0 mg/mL, 1.0 mg/mL, 0.5 mg/mL and 0.1 mg/mL were tested.

5 RESULTS

5.1 Comparison

Figure 5 gives a qualitative comparison of the measured receiver curves of the susceptometer that was used previously in [11] and of the proposed device (in red and blue, respectively). The figure

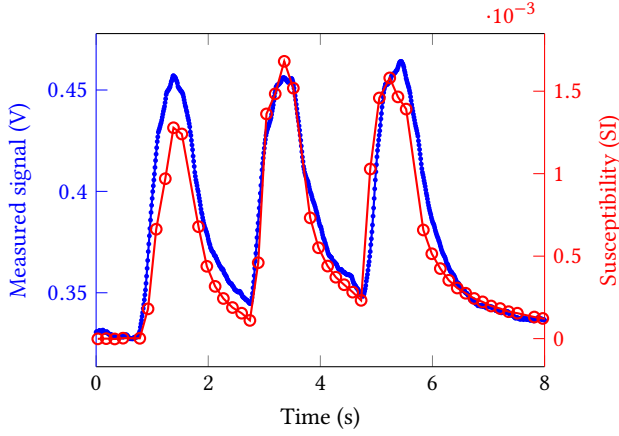


Figure 5: Comparison of measured curves by use of the commercial susceptometer that was previously used (red) and the proposed detector device (blue).

clearly demonstrates the increased resolution of the signal with the new detector.

Compared to the susceptometer, the sampling rate of the proposed detector of 100 samples/s is already 10 times larger. It was chosen due to restrictions of the ready to use graphical user interface (GUI) that accompanied the data acquisition card. With a customized data acquisition software, the sampling rate can further be increased.

5.2 Sequence transmission

The sample sequence “FAU” was successfully transmitted, as can be seen in Fig. 6. All bits were detected correctly using the simple method described in the previous section.

A second test with a random 80 bit sequence was performed, again with the optimal result of all peaks corresponding to a “1” being correctly detected (see Fig. 7).

A characteristic waveform for each burst of particles with a quick rise time and a delayed return to zero, as the particles are washed out of the detector coil by the background flow, can be observed. Due to the slow decay of particles in the tube because of laminar flow, successive bursts cause an accumulation of remaining particles which increases the measured concentration and further delays the return to zero, i. e., inter-symbol interference occurs.

5.3 Sensitivity Test

The measured signals for the six tested SPION suspension dilutions are shown in Fig. 8. The three peaks that were expected due to the transmitted binary sequence with three equispaced ones can be identified in all measurements except for the one with the lowest SPION concentration $c = 0.1$ mg/mL. The amplitudes scale with the concentration and range from 0.3 V ($c = 10$ mg/mL) to approx. 0.02 V ($c = 0.5$ mg/mL). For the considered setup the lowest concentration that allows safe detection of a bit is therefore determined as 0.5 mg/mL. Successful communication at lower concentrations may be possible but would require more robust equalization and coding schemes.

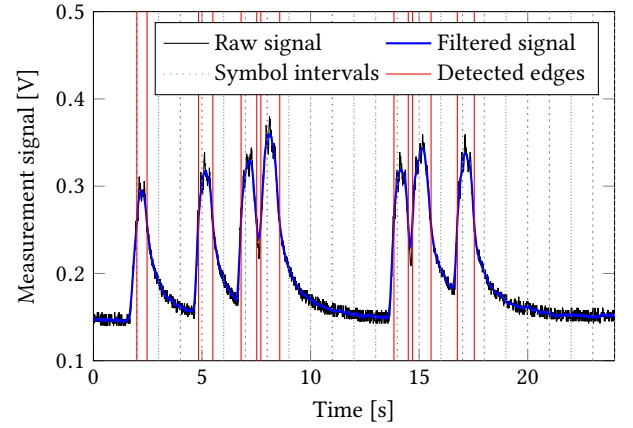


Figure 6: Transmission test with text sequence “FAU” (binary representation see (1)). Raw and filtered measurement signals are plotted in black and blue color, respectively. The symbol intervals, as derived from the first detected rising edge, are indicated by dotted gray vertical lines, detected edges by solid red lines. Sufficient values above the threshold are found in each symbol interval that corresponds to a binary “1”.

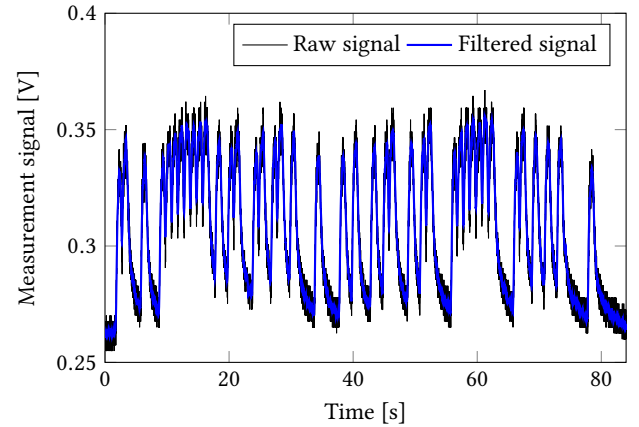


Figure 7: Transmission test with 80 bit random sequence (see (3)). Raw and filtered measurement signals are plotted in black and blue color, respectively. Each peak corresponding to a binary “1” can be clearly identified.

6 CONCLUSION

An optimized receiver for detection of superparamagnetic iron oxide nanoparticles in a molecular communication (MC) testbed was proposed. It was shown that the detector is capable of discriminating different particle concentrations that pass through the propagation channel, such that text messages and longer bit sequences can be effectively transmitted.

Compared to the previously used, commercial susceptometer, the proposed sensor device shows three advantages: First, it can be used with different detector coils, particularly custom made ones,

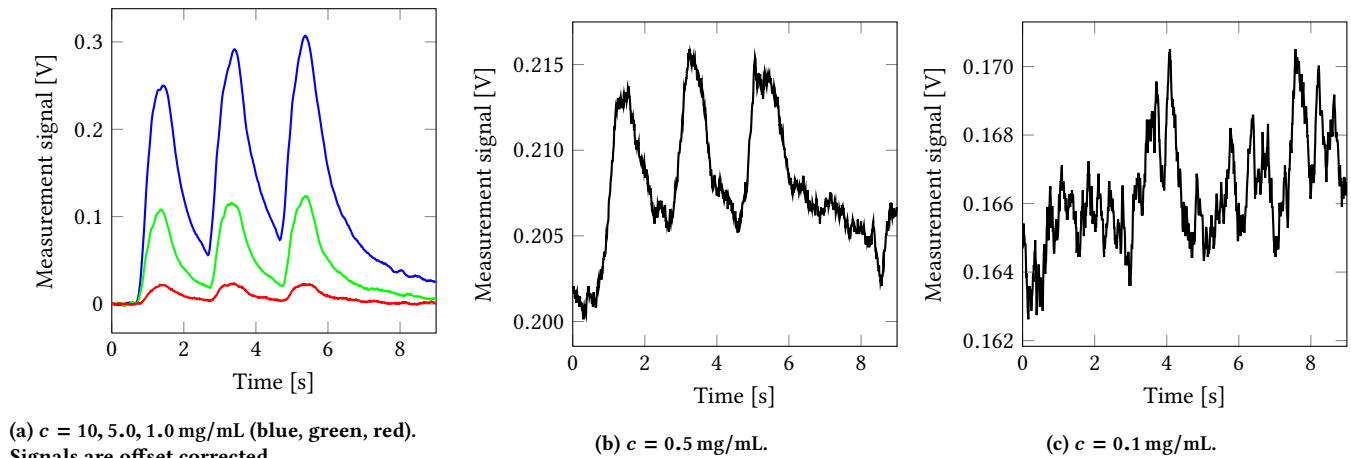


Figure 8: Sensitivity test. Measured series of three pulses for different particle concentrations $c = 10, 5.0, 1.0, 0.5, 0.1$ mg/mL.

which can be manufactured according to the dimensions of the MC testbed in use. Second, it provides an increased sample rate, which is currently limited by the software of the data acquisition card we used and which can be enhanced further by a custom made software. And third, the reference, a second coil that the detuning of the measurement coil is compared to, is made available for the user. In this way, on the one hand, conventional single-ended signaling can be implemented by fixing a tube with the channel medium (distilled water in our case) without particles as reference. On the other hand, differential signaling is now possible, too, by using two tubes as propagation channel: In this case, the transmitter encodes information in concentration differences of SPIONs between the two tubes rather than by particle injections into a single tube. This would open up new possibilities for transmitter designs, e. g., by steering particles into one tube or the other by magnetic fields, which would not suffer from the mechanical limitations of pumps and, in combination with a closed-loop system, from the need of a reservoir and a sink for the nanoparticles.

Therefore, the next steps of research includes the realization of a fully differential signaling testbed for molecular communication. Furthermore, the proposed sensor device will be evaluated and compared to the commercial susceptometer as well as to alternative measurement approaches, particularly with respect to bit error rates for different measurement setups. Finally, an optimized receiver will allow to improve the testbed design and to investigate appropriate encoding and decoding strategies in a more detailed manner than it has been possible so far.

ACKNOWLEDGMENTS

This work was supported in part by the Emerging Fields Initiative (EFI) of the Friedrich-Alexander-Universität Erlangen-Nürnberg (FAU), the STAEDTLER-Stiftung, and the German Federal Ministry of Education and Research (BMBF), project MAMOKO.

REFERENCES

- [1] Nilangshu K. Das, Sounak Dey, Sarbajit Pal, and Parthasarathi Barat. 2013. Innovative Instrumentation to Measure Magnetic Susceptibility. *IEEE Transactions on Magnetics* 49, 9 (Sep. 2013), 4965–4969. <https://doi.org/10.1109/TMAG.2013.2259247>
- [2] Bob Dobkin and Jim Williams (Eds.). 2011. *Analog Circuit and System Design: A Tutorial Guide to Applications and Solutions*. Elsevier. <https://doi.org/10.1016/B978-0-12-385185-7.00032-9>
- [3] Nariman Farsad, Weisi Guo, and Andrew W. Eckford. 2013. Tabletop Molecular Communication: Text Messages through Chemical Signals. *PLoS ONE* 8, 12 (Dec. 2013), 1–13. <https://doi.org/10.1371/journal.pone.0082935>
- [4] Nariman Farsad, David Pan, and Andrea Goldsmith. 2017. A Novel Experimental Platform for In-Vessel Multi-Chemical Molecular Communications. In *GLOBECOM 2017 - 2017 IEEE Global Communications Conference*. 1–6. <https://doi.org/10.1109/GLOCOM.2017.8255058>
- [5] Laura Grebenstein, Jens Kirchner, Renata S. Peixoto, Wiebke Zimmermann, Florian Irnstorfer, Wayan Wicke, Arman Ahmadzadeh, Vahid Jamali, Georg Fischer, Robert Weigel, Andreas Burkovski, and Robert Schober. 2019. Biological Optical-to-Chemical Signal Conversion Interface: A Small-Scale Modulator for Molecular Communications. *IEEE Transactions on NanoBioscience* 18, 1 (Jan 2019), 31–42. <https://doi.org/10.1109/TNB.2018.2870910>
- [6] Vahid Jamali, Arman Ahmadzadeh, Wayan Wicke, Adam Noel, and Robert Schober. 2019. Channel modeling for diffusive molecular communication – A tutorial review. <https://arxiv.org/abs/1812.05492> submitted for publication.
- [7] Bon-Hong Koo, Changmin Lee, H. Birkan Yilmaz, Nariman Farsad, Andrew W. Eckford, and Chan-Byoung Chae. 2016. Molecular MIMO: From Theory to Prototype. *IEEE Journal on Selected Areas in Communications* 34, 3 (March 2016), 600–614. <https://doi.org/10.1109/JSAC.2016.2525538>
- [8] Bhuvana Krishnaswamy, Caitlin M. Austin, J. Patrick Bardill, Daniel Russakow, Gregory L. Holst, Brian K. Hammer, Craig R. Forest, and Raghupathy Sivakumar. 2013. Time-Elapse Communication: Bacterial Communication on a Microfluidic Chip. *IEEE Transactions on Communications* 61, 12 (December 2013), 5139–5151. <https://doi.org/10.1109/TCOMM.2013.111013.130314>
- [9] Antje Lindemann, Ralph Pries, Kerstin LÄjdtke-Buzug, and Barbara Wollenberg. 2015. Biological Properties of Superparamagnetic Iron Oxide Nanoparticles. *IEEE Transactions on Magnetics* 51, 2 (Feb 2015), 1–4. <https://doi.org/10.1109/TMAG.2014.2358257>
- [10] Tadashi Nakano, Andrew W. Eckford, and Tokuko Haraguchi. 2013. *Molecular Communication*. Cambridge University Press, Cambridge. <https://doi.org/10.1017/CBO9781139149693>
- [11] Harald Unterwiesing, Jens Kirchner, Wayan Wicke, Arman Ahmadzadeh, Doaa Ahmed, Vahid Jamali, Christoph Alexiou, Georg Fischer, and Robert Schober. 2018. Experimental Molecular Communication Testbed Based on Magnetic Nanoparticles in Duct Flow. In *2018 IEEE 19th International Workshop on Signal Processing Advances in Wireless Communications (SPAWC)*. 1–5. <https://doi.org/10.1109/SPAWC.2018.8446011>
- [12] Linchen Wang, Nariman Farsad, Weisi Guo, Sebastian Magierowski, and Andrew W. Eckford. 2015. Molecular barcodes: Information transmission via persistent chemical tags. In *2015 IEEE International Conference on Communications (ICC)*. 1097–1102. <https://doi.org/10.1109/ICC.2015.7248469>